

A Multi-Objective Method to Design Demand Response Strategies for Power Systems including Wind Power Generation

Miadreza Shafie-khah
C-MAST/UBI, Covilha,
Portugal
miadreza@ubi.pt

Marta Ribeiro
FEUP, Porto,
Portugal
marta.francisca20@gmail.com

Neda Hajibandeh,
Gerardo J. Osório
C-MAST/UBI, Covilha, Portugal
hajibandeh.n@gmail.com;
gjosilva@gmail.com

João P. S. Catalão
INESC TEC and FEUP, Porto,
C-MAST/UBI, Covilha, and
INESC-ID/IST-UL, Lisbon,
Portugal
catalao@fe.up.pt

Abstract—The uncertainty and variability of renewable energy sources, wind energy in particular, poses serious challenges for the optimal operation and planning of power systems. In this paper, in order to obtain flexible market conditions while power generated by renewable units is short and supply and demand are imbalanced, a Demand Response (DR) strategy is studied to provide network requirements, because Demand Response Programs (DRPs) improve demand potential and increase security, stability and economic performance. The proposed hybrid model created by the integration of wind energy and DR using Time of Use (ToU) or Emergency DRP (EDRP) improves supply and demand. The problem is solved considering the Independent System Operator (ISO) and using a stochastic multiple-objective (MO) method. The objective is to simultaneously minimize the operation costs and the environmental pollution while assuring compliance of network security constraints and considering multiple economical and technical indexes.

Index Terms—Environmental emissions, Demand response, Stochastic programming, Renewable energy.

I. NOMENCLATURE

A. Indexes

b	Network bus
j	Load
i	Thermal unit
t	Hour
l	Transmission branch
s	Wind scenario
w	Wind farm
m	Segment for linearizing thermal unit's cost function

B. Parameters

ρ_t^0	Initial electricity price (\$/MWh)
d_{jt}^0	Initial electricity demand
$E_{tt'}$	Demand elasticity
DR^{max}	Maximum DR potential

A_t	Incentive rates (\$/MWh)
ρ_t	Electricity tariffs (\$/MWh)
P_i^{min}/P_i^{max}	Minimum/Maximum generation limit (MW)
MUT_i/MDT_i	Minimum up/down times of units
NLC_i	No load cost of units
RU_i/RD_i	Ramp up/down of units
SUC_i	Start-up cost of units
SUR_i/SDR_i	Spinning up/down reserves of units
C_{im}^e	Slope of segment m in linearizing cost function of units (\$/MWh)
C_i^{RU}/C_i^{RD}	Capacity of up/down reserve (\$/MW)
C_i^{ERU}/C_i^{ERD}	Energy of up/down reserve (\$/MWh)
$E_i^{SO_2}/E_i^{NO_x}$	Emission rates of SO_2 and NO_x (\$/kg)
X_l	Branches reactance
C_{wt}^{wind}	Wind farms cost
π_{cur}	Spillage wind cost
ω_s	Wind scenarios likelihood
$VOLL_j$	Value of lost load (\$/MWh)
$P_w^{install}$	Rated power of wind units (MW)
W_{wt}^{max}	Wind power available (MWh)
C. Variables	
F_{cost}	Expected operation cost (\$)
$F_{emissions}$	Emission (kg)
δ_{bts}	Voltage angle (rad)
F_{lts}	Power flow of branch l (MVA)
P_{itm}^e	Production of segment m of units (MWh)
C_{it}^{ST}	Start-up cost of units (\$)
P_{it}^{tot}	Scheduled production of units (MW)
P_{wt}^{wind}	Scheduled production of wind farms (MW)
SR_{it}^U/SR_{it}^D	Scheduled up/down reserves of units (MW)
P_{its}^{tot}	Total scheduled unit i power (MW)
sr_{its}^U/sr_{its}^D	Deployed up/down reserves of units (MW)

J.P.S. Catalão acknowledges the support by FEDER funds through COMPETE 2020 and by Portuguese funds through FCT, under Projects SAICT-PAC/0004/2015 - POCI-01-0145-FEDER-016434, POCI-01-0145-FEDER-006961, UID/EEA/50014/2013, UID/CEC/50021/2013, UID/EMS/00151/2013, and 02/SAICT/2017 - POCI-01-0145-FEDER-029803, and also funding from the EU 7th Framework Programme FP7/2007-2013 under GA no. 309048.

LS_{jts}	Compulsory load curtailment (MW)
W_{wst}^{spil}	Spilled power of wind farms (MW)
d_{jt}	Modified demand after applying DR programs
L_{jt}	Load after applying DR programs
L_t^{final}	Hourly load after applying DR programs
I_{it}	Commitment of units
y_{it}/z_{it}	Binary start-up/shutdown indicators

II. INTRODUCTION

With the introduction and increase of the utilization of the various renewable energy resources, a challenge is introduced in the planning of energy dispatch. Renewables are associated with uncertainty, so the amount of energy produced is hard to forecast, and the profile of renewable production does not match the profile of the electric demand, in general.

Due to all these reported aspects, deprivation of energy in certain periods can occur, as well as the excess of energy in others [1]-[3]. Increasing performance flexibility of the system is the key solution to balance these problems [4]. In order to increase system flexibility, novel mechanisms have been increasingly available, such as Demand Response (DR) programs [5], reinforcement of the network and the availability of fast generators [6], smart networks and electric vehicles [7] and also energy storage [8].

To this end, experiences of applying DR were analyzed and it was confirmed that Demand Response Programs (DRPs) are effective in providing more flexibility [9], allowing to reduce demands during peak loads [10].

Letting customers' potential be catalyzed by DR programs, it may be possible to create a new window of opportunities in increasing the flexibility of power systems, in the face of the variability of wind production or contingencies. Uncertainty of wind power using Security Constrained Unit Commitment (SCUC) [11] and the implementation of DRPs in SCUC problems [12]-[14] have attracted attentions.

Although various publications have addressed the renewable energy generation and demand response programs, the impact of a combination of price-based DRPs (PBDRPs) and incentive-based DRPs (IBDRPs) in renewable-based systems on the market power, reliability indices and market prices needs more attention.

A stochastic multi-objective problem is considered with wind energy integration and a DR strategy, which aims at the minimization of two objectives, operational costs for the ISO and air pollution. In the proposed model, the uncertainty of wind power production is modeled through various scenarios in the two-stage stochastic problem. Reserved energy is used to balance generation and consumption. For representing DR programs effects and market power changes, Energy Not Supplied (ENS), marginal price, Lerner index (LI) and load factor are analyzed.

III. THE PROPOSED MODEL

A. Model of DR Programs

DR may be explained as the change in the demand of the end users/consumers in relation to the average consumption of the electricity.

This change may occur as a consequence of changing the price of electricity over time, or the imposition of penalties or incentives, leading to shifting the consumption from time slots when the reliability of the system is at a high risk to valley or off-peak periods.

DRPs are split into two categories, called PBDRPs and IBDRPs [15].

The PBDRPs comprise time of use (TOU) program, real-time pricing (RTP), and critical peak pricing (CPP). These time-based DR schemes motivate end-users/consumers to decrease or shift their consumptions through implementing these programs and the corresponding modifications on electricity tariffs.

IBDRPs are categorized into two clusters, namely: classical and market based strategies. These strategies also induce consumers to change their normal consumption in return of a particular payment or "incentive" [16].

The economic load model and the demand side consumption after the application of DR programs is adopted from [17] as can be seen (1):

$$d(t) = d_0(t) \left\{ 1 + \sum_t \left[\frac{(E(t, t') \cdot (A(t) + (\rho(t) - \rho^0(t)))}{\rho^0(t)} \right] \right\} \quad (1)$$

B. Stochastic Multi-Objective Model

The proposed model is based in combining stochastic optimization with the ϵ -constraint multi-objective method. Wind farms generation is the only stochastic parameter considered, which is modeled using scenarios that enable taking into account the inconstancy characteristics of the wind speed.

The ϵ -constraint multiple-objective method minimizes two divergent objective functions simultaneously: minimization of utilization cost for ISO, on the one hand, and minimization of pollution rate of conventional generation units, on the other hand, as represented in (2):

$$\text{Minimize } \{F_{cost}, F_{emissions}\} \quad (2)$$

Each objective function is now defined in more detail, starting with the utilization cost for ISO, given by (3):

$$\begin{aligned} F_{cost} = & \sum_t \left\{ \sum_i \left[\left(NLC_i \cdot y_{it} + SUC_i + \sum_m (P_{it}^e(m) \cdot C_i^e(m)) \right) \right. \right. \\ & \quad \left. \left. + (C_i^{RU} \cdot SR_{it}^U + C_i^{RD} \cdot SR_{it}^D) \right. \right. \\ & \quad \left. \left. + \sum_w (C_{wt}^{\text{wind}} \cdot P_{wt}^{\text{wind}}) \right] \right\} \\ & + \sum_s \sum_t \omega_s \cdot \left\{ \sum_i [(C_i^{ERU} \cdot sr_{its}^U) - (C_i^{ERD} \cdot sr_{its}^D)] \right. \\ & \quad \left. + \sum_w (\pi_{spil} \cdot W_{wst}^{spil}) \right. \\ & \quad \left. + \sum_j (VOLL_j \cdot LS_{jts}) \right\} \end{aligned} \quad (3)$$

The cost function has two steps. The first step describes hourly decisions of conventional generation unit commitment and it is independent of scenarios.

Decision variables of renewable generation units do not change in this first step. Therefore, market clearing is performed for day-ahead market ignoring scenarios.

In the second step, probable wind generation cases are considered based on the probability of each case; the value of each decision variable in this step for each scenario is different based on wind intensity. The variables of this second step are the balanced market decision variables, which occur in real-time. The objective function for pollution rate is given as follows:

$$F_{\text{emission}} = \sum_i \sum_t [P_{it}^{\text{tot}} \cdot (E_i^{\text{SO}_2} + E_i^{\text{NO}_x})] \quad (4)$$

C. First Stage Constraints

The constraints for the first stage, day-ahead market, and independent of scenarios are considered as follow:

- DR constraints:

$$d_j(t) = DR^{\max} \cdot d_j^0(t).$$

$$\left(1 + \sum_t \left[\frac{(E(t, t') \cdot (A(t) + (\rho(t) - \rho^0(t)))}{\rho^0(t)} \right] \right) \quad (5)$$

$$L_j(t) = d_j(t) + (1 - DR^{\max}) \cdot d_j^0(t) \quad (6)$$

$$L^{\text{final}}(t) = \sum_j L_j(t) \quad (7)$$

Hourly demand after implementation of DR programs is represented in (5), where $A(t)$ is equal to 1 for incentive-based DRPs and it is 0 for time (price)-based DR programs. Load after implementation of DR at hour t and for each load index j is shown in (6). Equation (7) provides for every hour the final value for load after DR implementation.

- Startup Cost:

$$0 \leq SUC_i \leq C_{it}^{\text{ST}}(I_{it} - I_{i,t-1}) \quad (8)$$

- Max Scheduled Wind:

$$P_{wt}^{\text{wind}} \leq W_{wt}^{\max} \cdot P_w^{\text{install}} \quad (9)$$

- Max Scheduled Power/Reserve related to the Conventional Units:

$$P_{it}^{\text{tot}} + SR_{it}^U \leq P_i^{\max} \cdot I_{it} \quad (10)$$

$$P_{it}^{\text{tot}} - SR_{it}^D \geq P_i^{\min} \cdot I_{it} \quad (11)$$

The up and down reserve of thermal units are considered for the optimal performance of the system, handling the uncertainty of wind generation.

D. Second Stage Constraints

- Demand Balance in RT:

$$\sum_i (sr_{its}^U - sr_{its}^D) + \sum_j LS_{jts} + \sum_w (P_w^{\text{install}} - P_{wt}^{\text{wind}} - W_{wst}^{\text{cur}}) = \sum_l (F_{lts}) \quad (12)$$

$$F_{lts} = \frac{(\delta_{bts} - \delta'_b ts)}{X_l} \quad (13)$$

In order to preserve the security of the system and the power flow in each scenario, supply and demand balance should be satisfied for each bus.

- Load Shedding and Wind Spillage:

$$LS_{jts} \leq L_j(t) \quad (14)$$

$$W_{wst}^{\text{spli}} \leq P_{wt}^{\text{wind}} \cdot P_w^{\text{install}} \quad (15)$$

- Reserve Constraints of Thermal Units:

$$sr_{its}^U \leq SR_{it}^U \quad (16)$$

$$sr_{its}^D \leq SR_{it}^D \quad (17)$$

- Constraints for Reserve Limitations:

$$P_{its}^{\text{tot}} = P_{it}^{\text{tot}} + sr_{its}^U - sr_{its}^D \quad (18)$$

$$P_{its}^{\text{tot}} \leq P_i^{\max} \cdot I_{it} \quad (19)$$

$$P_{its}^{\text{tot}} \geq P_i^{\min} \cdot I_{it} \quad (20)$$

After describing objective function equations and system constraints, the MO function is modelled. Comparatively with single-objective problems, solving MO problems is more complex given the absence of a single solution. The set of solutions is selected among a wide range of solutions, representing the so-called Pareto front [18]. This pareto front enables decision makers to select the best solution from the wide range of possible solutions, favoring the optimal utilization of the system.

Table I shows a payoff table regarding the MO problem together with Pareto strategy.

The ϵ -constraint method is employed for obtaining the Pareto curve. First, the payoff table should be satisfied. This table describes problem optimization values for each objective function separately [19].

The augmented ϵ -constraint method can be considered as follows:

$$\text{Min} \left(F_{\text{cost}} - \delta \times \left(\frac{S_2}{r_2} \right) \right) \quad (21)$$

subject to: $F_{\text{emissions}} + S_2 = \varepsilon_2^k, S_2 \in R^+$

$$\varepsilon_2^k = F_{\text{max}}^{\text{Emission}} - \left(\frac{F_{\text{max}}^{\text{Emission}} - F_{\text{min}}^{\text{Emission}}}{q_2} \right) \times k, \quad k = 0, 1, \dots, q_2 \quad (22)$$

where:

δ denotes the scaling factor;

S_2 represents the slack variable;

$F_{\text{max}}^{\text{Emission}}$, $F_{\text{min}}^{\text{Emission}}$ denote the emission objective function max/min values extracted from payoff table, respectively;

ε_2^k represents the k -th range of $F_{\text{emissions}}$;

r_2 denotes total air pollution range;

q_2 represents number of the equal part;

The possibility of controlling problem density using variable q is one of the main advantages of this method. Compared to the ϵ -constraint method, the objective function increases by adding variable S_2 . The variable S_2 is substituted with $\delta \times (S_2/r_2)$ to avoid dimension problems, preventing the possibility of inefficient solutions.

IV. NUMERICAL STUDY

The efficiency of the DR programs is demonstrated in this paper by using the 24-bus IEEE system, which includes 26 generation units, 6 wind units, 24 buses, 17 loads and 5 transformers.

TABLE I: PAYOFF TABLE I

	\mathbf{F}^{Cost}	$\mathbf{F}^{\text{Emissions}}$
Min \mathbf{F}^{Cost}	$F_{\text{min}}^{\text{Cost}}$	$F_{\text{max}}^{\text{Emission}}$
Min $\mathbf{F}^{\text{Emissions}}$	$F_{\text{max}}^{\text{Cost}}$	$F_{\text{min}}^{\text{Emission}}$

TABLE II: CONVENTIONAL GENERATION UNITS ENERGY OFFERING DATA

Unit no.	Generation Power Segments (MW)						Energy offering information				Start-up cost (\$)	Emission rates (Kg/MWh)	
	P_i^{min}	$P_{it}^e(1)$	$P_{it}^e(2)$	$P_{it}^e(3)$	$P_{it}^e(4)$	P_i^{max}	$C_{it}^e(1)$	$C_{it}^e(2)$	$C_{it}^e(3)$	$C_{it}^e(4)$	C_{it}^{ST}	$E_i^{NO_x}$	$E_i^{SO_2}$
1-5	2.4	2.4	3.6	3.6	2.4	12	23.41	23.78	26.84	30.4	87.4	1.14	0.456
6-9	15.8	15.8	0.2	3.8	0.2	20	29.58	30.42	42.82	43.28	15	0.832	0.333
10-13	15.2	15.2	22.8	22.8	15.2	76	11.46	11.96	13.89	15.97	715.2	3.125	1.25
14-16	25	25	25	30	20	100	18.6	20.03	21.97	22.72	575	1.85	0.74
17-20	54.25	54.25	38.75	31	31	155	9.92	10.25	10.68	11.26	312	2.602	1.041
21-23	68.95	68.95	49.25	39.4	39.4	197	19.2	20.32	21.22	22.13	1018.9	3.26	1.304
24	140	140	87.5	52.5	70	350	10.08	10.66	11.09	11.72	2298	8.333	3.333
25-26	100	100	100	120	80	400	5.31	5.38	5.53	5.66	0	0	0

Wind units are located at buses 1, 4, 6, 18, 21 and 22. Each wind unit generates 150MW and the total generated power by wind is 900MW. For the modeling of the wind behavior, a Rayleigh distribution function for wind speed was considered, and the same strategy was utilized to determine the wind power production. To cover all the possibilities, a wide range of scenarios were generated through Roulette Wheel Mechanism (RWM).

All generated scenarios were decreased to the 10 more probable scenarios to mitigate the computation time. The scenario reduction method alleviates complexity, making the models easier to manage. The employed scenarios are depicted in Fig. 1. The probability of all scenarios is assumed to be 10%. Moreover, the wind spillage cost in each scenario is considered to be equal to 40 \$/MWh.

Thermal units offer their price proposals to the market operator in three steps. The data regarding the power generated by thermal units, fuel cost of units, cost and pollution rate of each generation unit are given in Table II. A total of 26 generators has been considered. The VOLL is assumed to be equal to 100 \$/MWh, which means that for each loss of 1 MWh due to involuntary load shedding during the operation, the market operator must pay 100\$ to the affected customer.

A. Modeled Alternatives

The EDRP program is an incentive-based program and ToU is a price-based program; an integration of these programs is considered to research about the effect of applying DR programs. The tariffs of these programs are given in Table III. The initial value of electricity cost in this model is obtained using average value of market price before implementing DR programs. This value if 15\$/MWh. The incentive of EDRP at peak hours is also considered to be 15\$/MWh.

Accordingly, seven diverse alternatives were determined, as shown in Table IV. Alternative 1 is the base one, disregarding DRP; besides, the electricity tariff is considered fixed during 24 hours. In Alternative 2, ToU is modeled with 10% of consumer's contribution, whereas in Alternative 3 this value has been changed to 20%. In relation to Alternative 4 and Alternative 5, the EDRP is implemented with a variant level of consumer's contribution coefficient, 10 and 20%, respectively. Alternatives 6 and 7 consider both ToU and EDRP with 10 and 20% DRP participation, respectively.

The ϵ -constraint method is performed in 65 iterations. The payoff table values are found by considering the objective function optimization, and they are given in Table V.

As expressed before, in a multi-objective approach the augmented ϵ -constraint method has as the key function of generating the Pareto front, which in turn will enable the selection of the most feasible solution. The market operator is expected to take part in the decision-making process.

With this aim, several indexes are employed to analyze the capability of DRPs.

The indexes are considered as below:

- Load Factor:

$$LF = (\text{Mean demand}/\text{Max Demand}) \times 100;$$
- Marginal Price;
- Energy Not Supplied:

$$ENS = \sum_j \sum_t \sum_s (LS_{jts});$$
- Lerner Index:

$$Lerner = (\text{Price} - \text{Margi Cost})/\text{Price}$$

B. Alternatives 1, 2 and 3

In this subsection, the first three alternatives have been analyzed: the base alternative and TOU programs with 10 and 20% of demand side contribution level.

When the Pareto solutions are achieved, the optimal solution is chosen for each alternative from the viewpoint of the system operator. Satisfying the ISO, the allowed limits of the emission (less than 150 tons) should be ensured. Afterwards, the solutions that stay within limit have to be verified, and the one having the smallest value is chosen.

Fig. 2 depicts the Pareto curves, and the desirable points chosen are diagnosed in red.

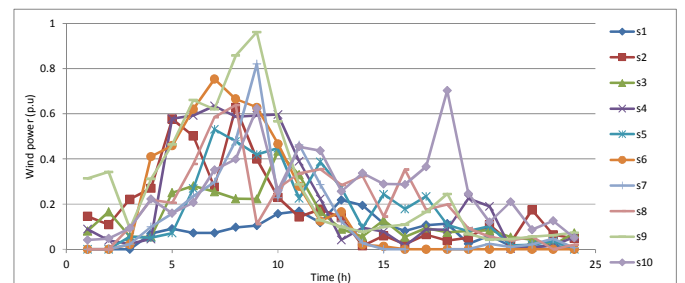


Figure 1. Considered wind power generation scenarios.

TABLE III: DRP'S TARIFFS (\$/MWh)

DRP	Valley (t_1-t_8)	Off-peak (t_9-t_{16})	Peak ($t_{17}-t_{24}$)
<i>Base alternative</i>	15.0	15.0	15.0
<i>TOU</i> program	7.5	15.0	30.0
<i>EDRP</i> program	15.0	15.0	15.0
<i>TOU+EDRP</i> program	7.5	15.0	30.0

TABLE IV: THE STUDIED ALTERNATIVES

Alternative	DR strategy	Participation coefficients in DRPs (%)
1	Base alternative	0
2	TOU program	10
3	TOU program	20
4	EDRP program	10
5	EDRP program	20
6	TOU+EDRP program	10
7	TOU+EDRP program	20

TABLE V: PAYOFF TABLE II

	$F^{Cost}(\$)$	$F^{Emissions}$ (kg)
Min F^{Cost}	438708.1	259063.3
Min $F^{Emissions}$	2932832.5	138212.7

For the base alternative, the selected solution corresponds to 148913.3 kg and 576248.2 \$; for Alternative 2, the selected solution has the values of 148501.7 kg and 536773.1 \$; finally, for Alternative 3, the selected solution has the values of 146251.8 kg and 518421.4 \$. It should be expressed that the cost decreased about 6% for Alternative 2 in relation to the base alternative. With the further increase of the client's participation, to 20% in Alternative 3, the cost decreased even more, up to 10%.

In Fig. 3, the demand pattern is presented for 24 hours for the 3 alternatives. A reduction of the electric demand is verified in relation to the base alternative during the peak period due to the increase of the electric tariff (15 \$/MWh to 30 \$/MWh), from 17h to 24h. With 20% of customers' contribution, the modifications become even more relevant.

The load factor index for the 3 alternatives was therefore calculated, being 82.9%, 89.3% and 87.3% for alternatives 1, 2 and 3, respectively. The marginal prices are depicted in Fig. 4. Marginal prices have dropped dramatically considering TOU.

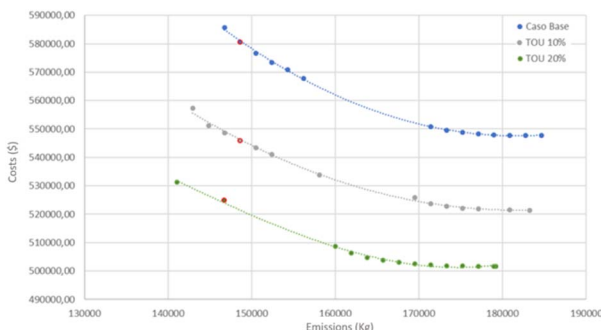


Figure 2. Pareto front (Alternatives 1, 2, and 3).

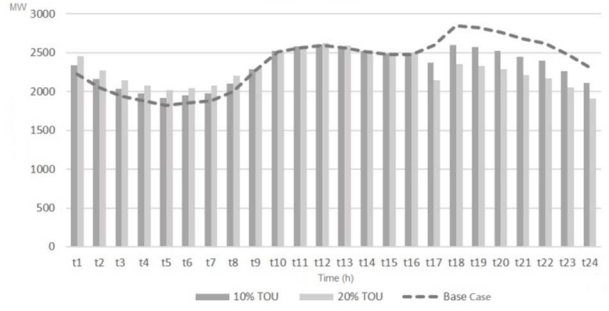


Figure 3. Demand curve (Alternatives 1, 2 and 3).

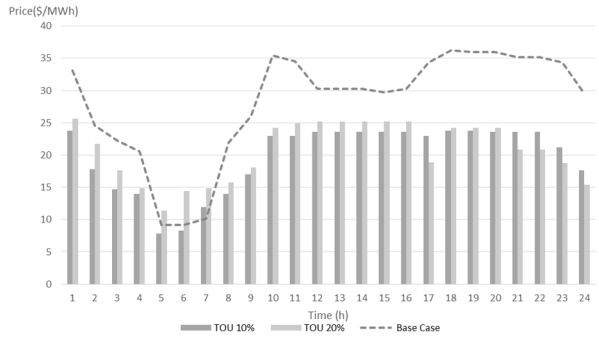


Figure 4. Marginal prices for 24 hours (Alternatives 1, 2, and 3).

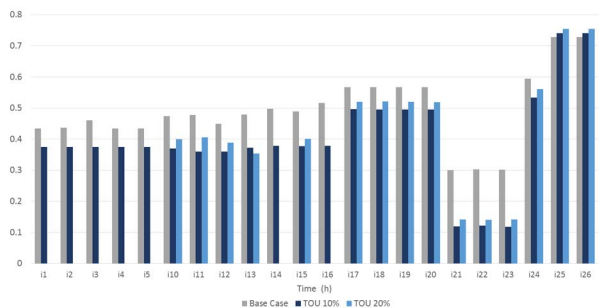


Figure 5. Lerner index of power plants (Alternatives 1, 2 and 3).

For the base alternative the amount for ENS index yields 21.2 MWh. Now, for 10 and 20% demand side coefficient in the TOU program, the ENS index decreased to 18.2 MWh and 12.2 MWh, respectively. Regarding the Lerner index, the results are shown in Fig. 5.

C. Alternatives 1, 4, and 5

In this part, the indexes for the EDRP strategy are analyzed, which have the same tariff like the base alternative (15\$/MWh). Notwithstanding, the incentive payment with a similar value to the tariff is considered if a decrease is carried out during peak hours.

The selection of the optimal solution from the Pareto set (depicted in Fig. 6) allows evaluating the indexes. The amount of the emissions is identical for the 3 alternatives, 148622.1 kg, because it correlates to the first solution to respect the max allowed limit of air pollution, thus being less than 150 tons.

In regards to the cost, with 10% contribution coefficient in EDRP, the cost value is 541752.2 \$, a reduction of about 7% in relation to the base alternative.

For the EDRP strategy with the participation coefficient equal to 20%, the cost amount declines to 515012.3\$, up to 11% compared with base alternative cost. According to Fig. 7, it can be possible to analyze the modifications in the load profile by implementing EDRP. The load factor corresponds to 88.1% and 85.4% for Alternatives 4 and 5, respectively, which are amounts larger than the base alternative (about 82.9%), demonstrating that these two alternatives shape the load curve flatter.

There is a decrease in the peak price with diverse types of EDRP, with the price diminishing more than the base alternative for all time slots, as shown in Fig. 8. Regarding ENS, as previously observed, the value is 20.8 MWh for the base alternative. With the participation coefficient of 10% for the EDRP program a reduced amount was obtained for the ENS, 18.2 MWh. Regarding LI, Fig. 9 shows that with the implementation of the EDRP program the number of the thermal units employed has decreased compared to the base alternative, as the demand decreases in peak hours.

D. Alternatives 1, 6 and 7

The combination of the two DR programs at the same time, TOU and EDRP, is now evaluated. The demand side participants are inspired to modify the demand patterns by price changes from the TOU strategy and through incentive payments for the sake of implementing the EDRP program. The Pareto front is shown in Fig. 10.

The optimum solution of Alternative 6 is equal to 146562.0 kg for emission and 516398.1 \$ for cost, whereas for Alternative 7 the emission and cost amounts yield 148548.8 kg and 476179.9 \$, respectively. This mixture of strategies creates a substantial cost decrease, approximately 11% for Alternative 6 and 18% for Alternative 7.

Analyzing Fig. 11, there is also a significant reduction in electricity demand during the peak hours compared with the base alternative.

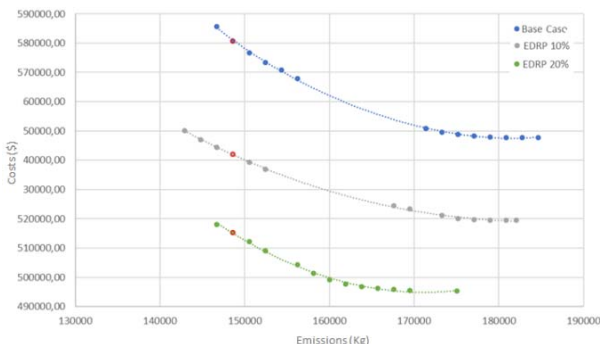


Figure 6. Pareto front for Alternatives 1, 4 and 5.

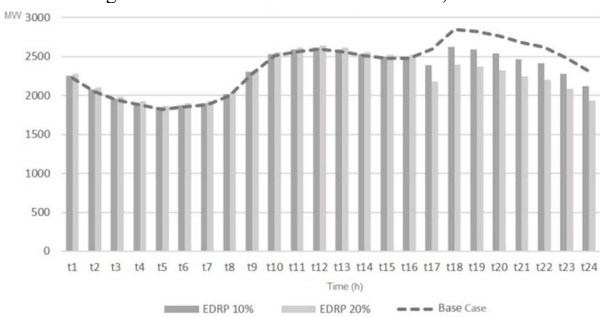


Figure 7. Demand profiles for Alternatives 1, 4 and 5.

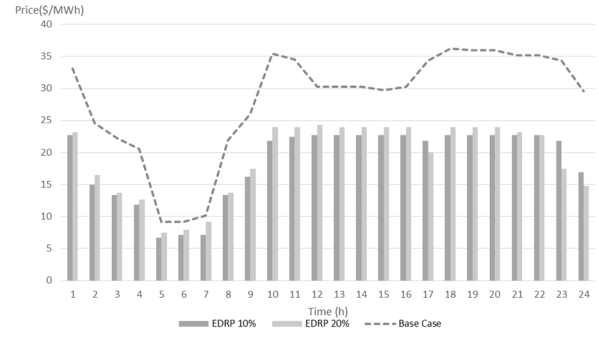


Figure 8. Marginal prices in 24 hours (Alternatives 1, 4, and 5).

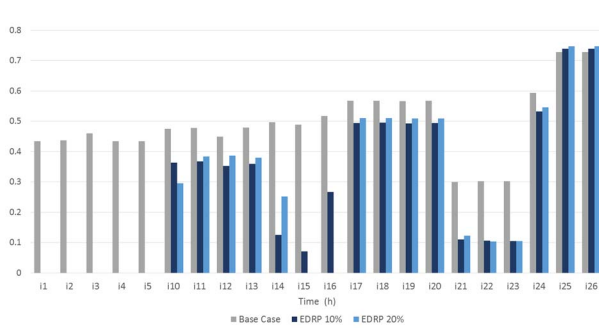


Figure 9. Lerner index of the power plants (Alternatives 1, 4 and 5).

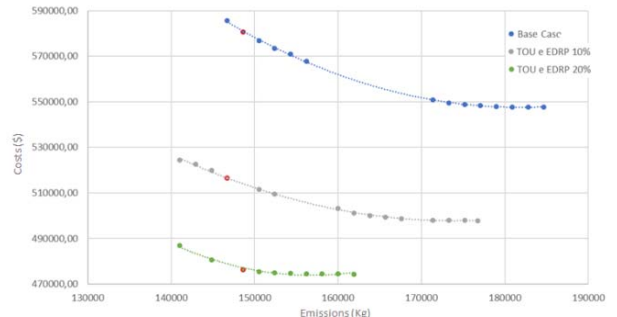


Figure 10. Pareto front for Alternatives 1, 6 and 7.

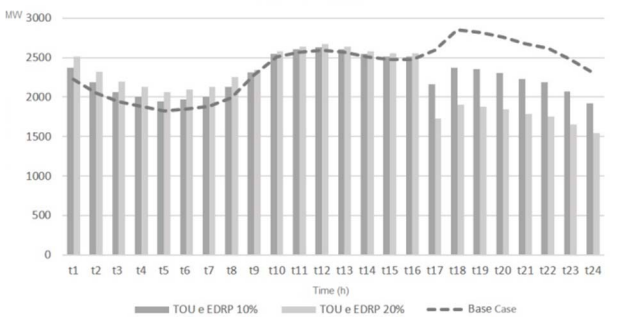


Figure 11. Demand profiles for Alternatives 1, 6 and 7.

The value of the load factor for Alternative 6 is 86.3%, and for alternative 7 it is approximately 81.7%. However, at certain times there is a slight price increment as a result of heightened demand, as seen in Fig. 12. Moreover, when analyzing the LI of each generator, Fig. 13, it can be observed that the value was noticeably reduced, and some thermal units were not even required when employing the DRPs.

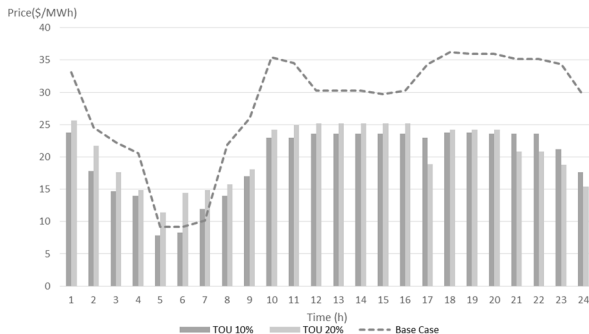


Figure 12. Marginal prices in 24 hours (Alternatives 1, 6 and 7).

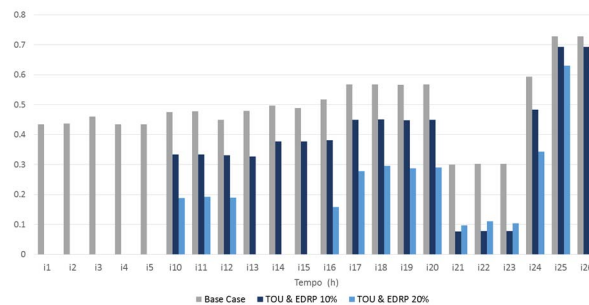


Figure 13. Lerner index of the power plants (Alternatives 1, 6 and 7).

V. CONCLUSION

In this paper, besides the modeling of DRPs, the integration of renewable energies was considered. In addition, it was intended to simultaneously minimize two objective functions: the minimization of costs for the system operator and the reduction of polluting gases emissions. A reduction in demand happens during peak hours with recovery for valley and off-peak hours, promoting a flat load curve. With the increase of the participation coefficient, the decrease in peak hours, as well as the increase in valley hours, had more impact. The proposed model could improve the load factor up to 6%. One of the great benefits of this model was the reduction of the marginal price by modifying electricity load for hours of lower demand and the reduction of the electricity consumption during hours of high prices. Another benefit was the decrease of ENS, which would lead to fewer interruptions. Moreover, the operation cost decreased up to 18%. In terms of market power, improvements were also observed, because the LI achieved for the varied alternatives under study was close to zero. Therefore, the implementation of DRPs in electric power systems with wind power potential allows increasing the operational flexibility of the system, minimizing ISO costs and reducing pollutant emissions.

REFERENCES

- [1] K. Friederich, C. Roesener. "A closer look on load management," in: *Proc. 5th IEEE Int. Conf Industrial Informatics*, 2007. Vol. 2.
- [2] N. Hajibandeh, M. Shafie-khah, S. Talari, J. Catalão. "The Impacts of Demand Response on the Efficiency of Energy Markets in Presence of Wind Farms", in: *Proc. Advanced Doctoral Conference on Computing, Electrical and Industrial Systems*, Springer, 2017.
- [3] N. Hajibandeh, M. Shafie-khah, G. Osório, J. Catalão. "A new approach for market power detection in renewable-based electricity markets" in: *Proc. 17th IEEE International Conference EEEIC*, 2017.
- [4] M. Shafie-khah, et al., "Strategic offering for a price-maker wind power producer in oligopoly markets considering demand response exchange," *IEEE Trans. Ind. Inform.*, vol. 11, no. 6, pp. 1542-1553, 2015.
- [5] P. S. Moura, A. T. De Almeida, "The role of demand-side management in the grid integration of wind power," *App. Energy*, vol. 87, no. 8, pp. 2581-2588, 2010.
- [6] D. Todd, et al., "Providing reliability services through demand response: A preliminary evaluation of the demand response capabilities of alcoa inc," *ORNL/TM 233*, 2008.
- [7] D. Dallinger, and M. Wietschel, "Grid integration of intermittent renewable energy sources using price-responsive plug-in electric vehicles," *Renew. Sust. Energy Rev.*, vol. 16, no. 5, pp. 3370-3382, 2012.
- [8] B. Dunn, H. Kamath, and J.-M. Tarascon, "Electrical energy storage for the grid: A battery of choices," *Science*, vol. 334, no. 6058, pp. 928-935, 2011.
- [9] H. Holttinen, et al., "The flexibility workout: managing variable resources and assessing the need for power system modification," *IEEE Power Energy Magazine*, vol. 11, no. 6, pp. 53-62, 2013.
- [10] P. Cappers, C. Goldman, D. Kathan, "Demand response in US electricity markets: Empirical evidence," *Energy*, vol. 35 no. 4, pp. 1526-1535, 2010.
- [11] D. Pozo, and J. Contreras, "A chance-constrained unit commitment with an $n - K$ security criterion and significant wind generation," *IEEE Trans. Power Syst.*, vol. 28, no. 3, pp. 2842-2851, 2013.
- [12] M. Parvania, M. Fotuhi-Firuzabad, "Demand response scheduling by stochastic SCUC," *IEEE Trans. Smart Grid*, vol. 1, no. 1, pp. 89-98, 2010.
- [13] A. Khodaei, et al. "SCUC with hourly demand response considering intertemporal load characteristics," *IEEE Trans. Smart Grid*, vol. 2, no. 3, pp. 564-571, 2011.
- [14] N. Hajibandeh, M. Shafie-khah, G.J. Osório, J. Aghaei, J.P.S. Catalão, "A heuristic multi-objective multi-criteria demand response planning in a system with high penetration of wind power generators," *App. Energy*, vol. 212, pp. 721-732, 2018.
- [15] B. P. Teimourzadeh, et al., "Customer behavior based demand response model," in: *Proc. IEEE Power Energy Society General Meeting*, 2012.
- [16] N. Hajibandeh et al., "The Mutual Impact of Demand Response Programs and Renewable Energies: A Survey," *Energies*, vol. 10, no. 9, 2017.
- [17] H. A. Aalami, M. Parsa Moghaddam, G. R. Yousefi, "Demand response modeling considering interruptible/curtailable loads and capacity market programs," *App. Energy*, vol. 87, no.1, pp. 243-250, 2010.
- [18] P. Ngatchou, A. Zarei, A. El-Sharkawi, "Pareto multi objective optimization," in: *Proc. 13th IEEE Inter. Conf. Intell. Syst. Appl. Power Syst.*, pp. 84-91. 2005.
- [19] A. R. Malekpour, et al., "Multi-objective stochastic distribution feeder reconfiguration in systems with wind power generators and fuel cells using the point estimate method," *IEEE Trans. Power Syst.*, vol. 28, no 2, pp. 1483-1492, 2013.